Photonik
Ingenieurbüro
Dr. Walter Luhs

PE-0600 Optical Interferometer

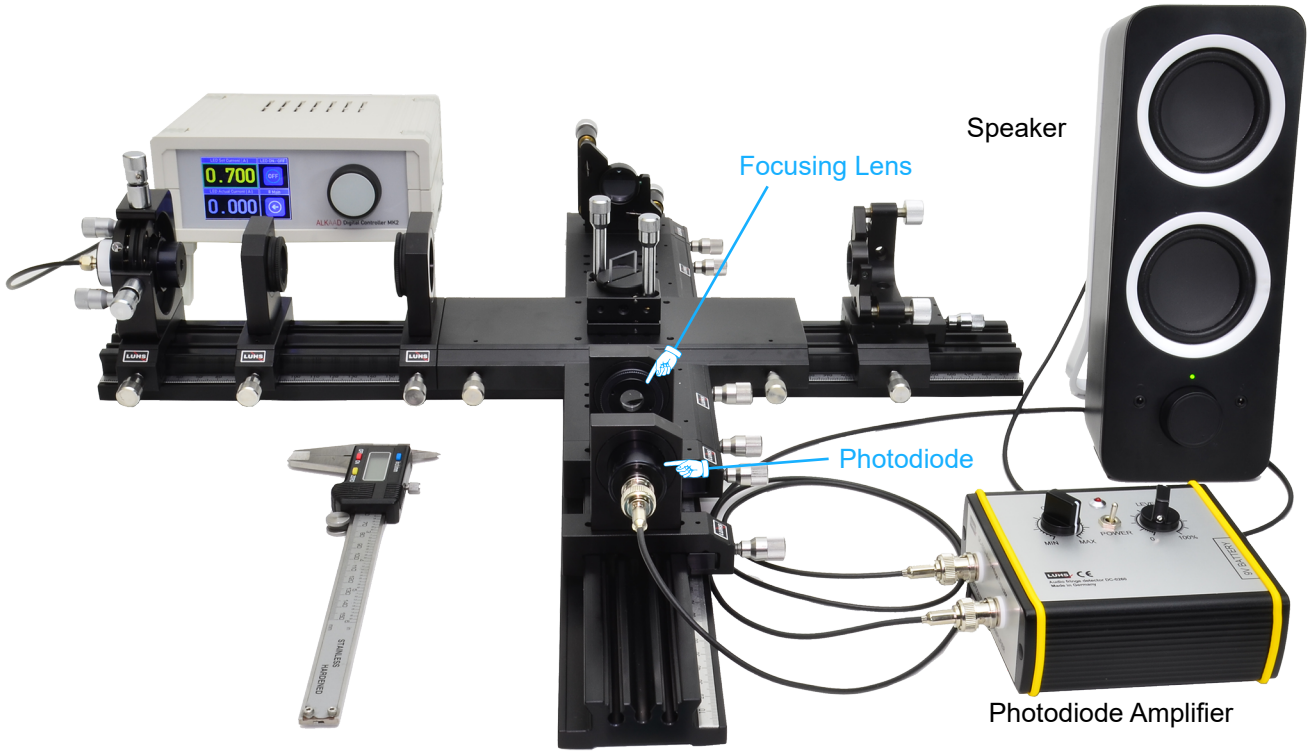

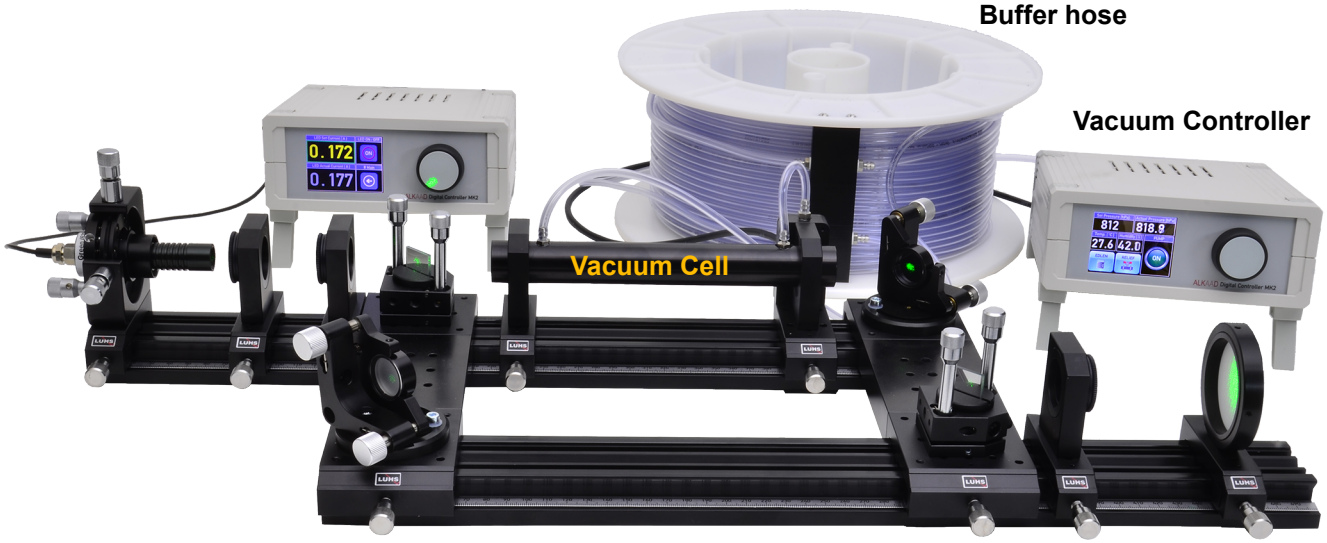

Table of Contents

1.0 Introduction

Interferometry plays an important role in the advancement of physics, and also has a wide range of applications in physical and engineering measurement.
Measuring is the process of comparing an unknown dimension with as known standard.
Thus a common accepted standard is required, like the standard for the length, the metre:

"The unit of length is the metre, defined by the distance, at 0°, between the axes of the two central lines marked on the bar of platinum–iridium kept at the Bureau International des Poids et Mesures and declared Prototype of the metre by the 1st Conférence Générale des Poids et Mesures, this bar being subject to standard atmospheric pressure and supported on two cylinders of at least one centimetre diameter, symmetrically placed in the same horizontal plane at a distance of 571 mm from each other."

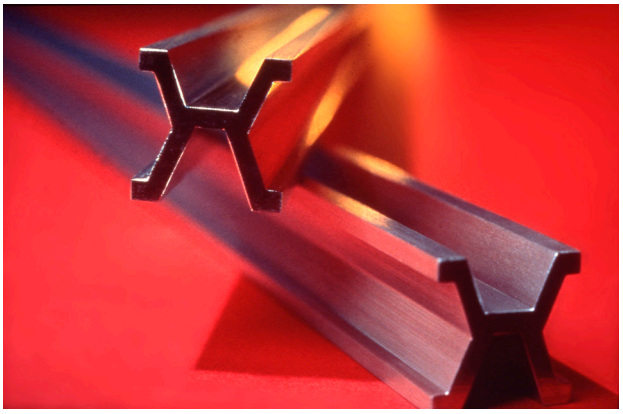

Fig. 1: Definition of the metre by a platinum-iridium bar

A better definition of the metre was defined on the 11th CGPM (General Conference on Weights and Measures) in 1960:
The metre is the length equal to 1 650 763.73 wavelengths in vacuum of the radiation corresponding to the transition between the levels 2p10 and 5d5 of the krypton 86 atom.
To transfer the definition of the length into a workshop an special apparatus was needed, the optical interferometer.

The krypton-86 discharge lamp operating at the triple point of nitrogen (63.14 K, −210.01 °C) was the state-of-the-art light source for interferometry in 1960, but it was soon to be superseded by a new invention: the laser, of which the first working version was constructed in the same year as the redefinition of the metre. Laser light is usually highly monochromatic, and is also coherent (all the light has the same phase, unlike the light from a discharge lamp), both of which are advantageous for interferometry.
The latest definition of the metre is the length *L* of the path travelled by light in vacuum during a time interval of 1⁄299,792,458 of a second.

$$L = c \cdot t$$

The speed of light in vacuum c is fixed to be 299,792,458 [m·s^{-1}], where the second is defined based on the caesium frequency $\Delta\nu_{Cs}$(9,192,631,770 Hz).

The definition of the metre is now bound to time and fixed speed of light. That means that if we have a light source with a known wavelength λ (or frequency υ) we can perform high precision length measurements independent where we are and independent of any other standard. The result of such the measurement will be:

$$L = N \cdot \lambda_{vac}$$

where N is the number of wavelength we detected and λ_{vac} is the wavelength in vacuum.
Typically we perform the measurements not in vacuum, thus the we need to use the relation

$$\lambda_{air} = n \cdot \lambda_{vac},$$

where n is the index of refraction of the environment, typically air. We introduce the Edlen formula, which provides a good approximation by measuring the pressure (p), temperature (T) and humidity (H) of the air:

$$n_{air} = f(p, T, H)$$

A device which can detect numbers of wavelength or even fractions of it, is for instance an interferometer.

That is why we are introduce such an apparatus which can measure distances with an extreme high precision. The attainable precision depends on the precision of the laser wavelength we are using.

In the experiment we use a standard frequency doubled Nd:YAG laser emitting a wavelength at 532 nm. The accuracy and precision is not crucial, since we are focussing on the fundamentals and practical demonstration, however it will be in the range of

$$\frac{dL}{L} \approx 10^{-6}$$

The typical arrangement to demonstrate the measurement of distances is a Michelson interferometer. In addition we introduce the Mach - Zehnder arrangement to measure the index of refraction of air.
While white light interferometry is certainly not new, combining rather old white light interferometry techniques with modem electronics, computers, and software has produced extremely powerful measurement tools. Within the scope of this experiments we will operate the Michelson interferometer also with a white light source.

2.0 Fundamentals

2.1 Characteristics of light

Light, the giver of life, has always held a great fascination for human beings. It is therefore no coincidence that people have been trying to find out what light actually is for a very long time. We can see it, feel its warmth on our skin, but we cannot touch it. The ancient Greek philosophers thought light was an extremely fine kind of dust, originating in a source and covering the bodies it reached. They were convinced, that light was made up of particles. As humankind progressed and began to understand waves and radiation, it was proved that light did not, in fact, consist of particles, but that it is electromagnetic radiation with the same characteristics as radio waves. The only difference is in the wavelength. We now know that the characteristics of light are revealed to the observer depending on how he sets up his experiment. If the experimenter sets up a demonstration apparatus for particles, he will be able to determine the characteristics of light particles. If the apparatus is one used to show the characteristics of wavelengths, he will see light as a wave. The question we would like to be answered is: What is light in actual fact? The duality of light could only be understood using modern quantum mechanics. Heisenberg showed, with his famous "uncertainty relation", that strictly speaking, it is not possible to determine the place x and the impulse p of any given occurrence at the same time

$$\Delta x \cdot \Delta p_x \geq \frac{1}{2}\hbar$$

If, for example, the experimenter chooses a set up to examine particle characteristics, he will have chosen a very small uncertainty of the impulse px. The uncertainty of x will therefore have to be very large and no information will be given on the course of the occurrence. The uncertainty is not given by the measuring apparatus, but is of basic nature. This means that light always has the particular property, the experimenter wants to measure. We can find out about any characteristic of light as soon as we think of it. Fortunately the results are the same, whether we work with particles or wavelengths, thanks to Einstein and his famous formula:

$$E = m \cdot c^2 = \hbar \cdot \omega$$

The equation states, that the product of the mass m of a particle with the square of its speed c relates to its energy E. It also relates to the product of Plank's constant and its radian frequency.

In further discussions of the fundamentals, we will use the wave representation and describe light as electromagnetic radiation. All types of this radiation, whether as radio waves, X-ray waves or light waves consist of a combination of an electrical field $\vec{E}$ and a magnetic field $\vec{H}$. Both fields are bound to each other and are indivisible. Maxwell formulated this observation in one of his four equations, which describe electromagnetic fields

$$\nabla \times \vec{H} \approx \frac{\partial \vec{E}}{\partial t}$$

According to this equation, every temporal change in an electrical field is connected to a magnetic field (Fig. 2).

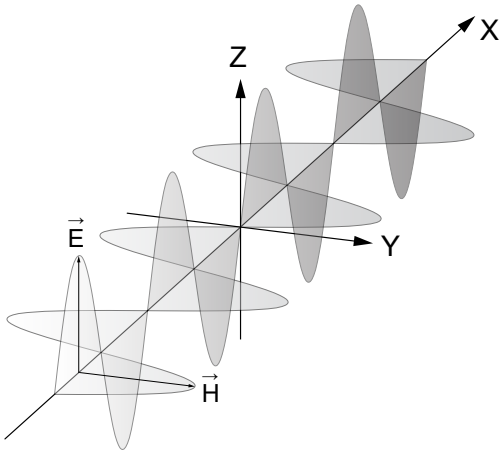

Fig. 2: Light as electromagnetic radiation

Due to the symmetry of this equation, a physical condition can be sufficiently described using either the electrical or the magnetic field. A description using the electrical field is preferred since the corresponding magnetic field can be obtained by temporal differentiation. In the experiments (as presented here) where light is used as electromagnetic radiation, it is advantageous to calculate only the electrical fields since the light intensity is:

$$I = \frac{c \cdot \varepsilon}{4\pi} \cdot \left|\vec{E}\right|^2$$

This is also the measurable property as perceived by the eye or by a detector. The speed of light is c in the respective medium and e is the corresponding dielectric constant. Since we are comparing intensities in the same medium, it is sufficient to use

$$I = \left|\vec{E}\right|^2$$

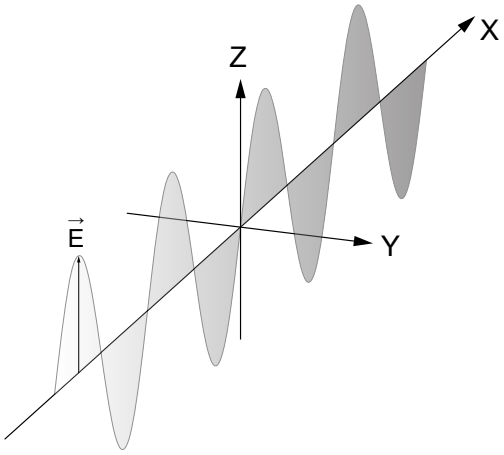

Fig. 3: In this experiment we need only consider the electrical field strength $\vec{E}$

The experimental findings agree with the theory of electromagnetic radiation (Maxwell), if the temporal behaviour of the field strength of the light $\vec{E}$ is a harmonic periodic function. In its simplest form this is a sine or cosine function. An amplitude E_0 and a wavelength λ should be used in the definition of this kind of function. Let us begin with the equation:

$$E_X = E_0 \cdot \sin\left(\frac{2 \cdot \pi}{\lambda} \cdot x\right), \qquad \textbf{(1)}$$

Theory

which we will elaborate and explain further.

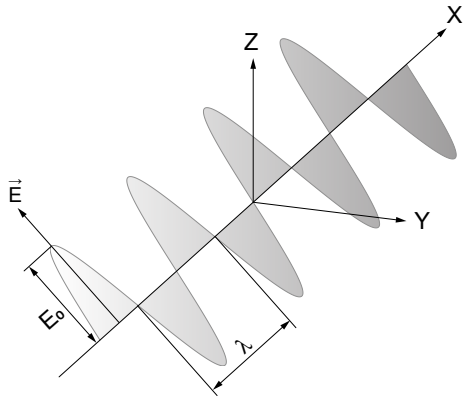

Fig. 4: Amplitude and wavelength

In the above figure, the light wave no longer oscillates in the Z-direction as in Fig. 3 but at a certain angle to the Z- or Y-axis. The X-axis has been chosen as the direction of propagation of the wave. We still require information on the direction in which the electrical field strength E_x oscillates to complete the description of the wave. Strictly speaking, the field E_x oscillates vertically to the direction of propagation X. However, we have to give information regarding the Z- and Y-axis. It leads to the term 'Polarisation' and Direction of Polarisation. In Figs. 2 and 3 we used linearly polarised light with a polarisation direction in Z and in Fig. 4 we used a different direction. We will now introduce the polarisation vector P, which is defined in the following Fig. 5. We look into the light wave in the direction of the X-axis for this purpose.

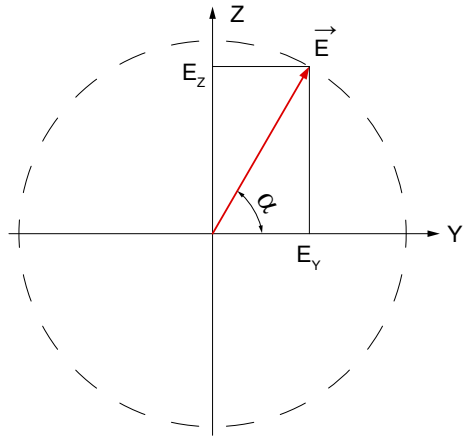

Fig. 5: Definition of the polarisation vector

We observe a wave propagating in the X-direction and oscillating at the electrical field amplitude E_0 under an angle of α to the Y-axis. The amplitude E_o is separated into its components, which oscillate in the Z- or Y-direction. We now write $\vec{E}$ as vector to indicate, that the electric field strength is now made up of individual components.

$$\vec{E} = E_x \cdot \vec{e}_x + E_x \cdot \vec{e}_y$$

Where $\vec{e}_z = (0,1)$ and $\vec{e}_y = (0,1)$ are the unit vector in the Z- or Y-direction in the ZY-plane. The unit vectors have the property of $|\vec{e}_z|=1$ and the scalar product $\vec{e}_y \cdot \vec{e}_z = 0$. The equation (1) can be generalised to:

$$E_X(Y,Z) = \left(E_0^Y \cdot \vec{e}_y + E_0^Z \cdot \vec{e}_z\right) \cdot \sin\left(\frac{2\pi}{\lambda} \cdot x\right)$$

At this point we come across a fundamental principle in classic wave theory, i.e. the principle of superimposition. A big word for the simple statement:

Every wave can be represented as the sum of individual waves.

In our example we had separated the wave as shown in Fig. 5 into two individual waves, i.e. one that oscillates in the Z-direction and another in the Y-direction. We could just as well say, the wave is created by the superimposition out of these two individual waves. The word ***interference*** can also be used to mean superimposition. In this context the wave is formed by the interference of two individual waves. We are using this definition, because it simplifies the written work.

2.2 Superimposition, phase and beat frequency

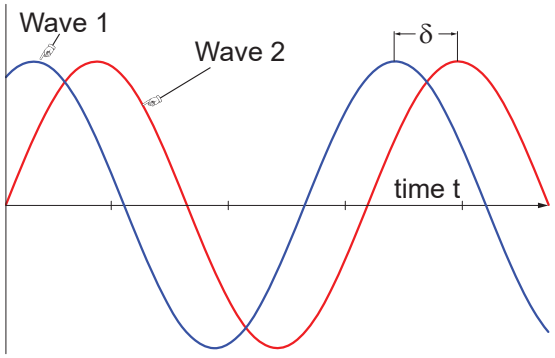

Fig. 6: Two waves with same frequency, but with a phase shift between each other

Obviously the phase δ contains information about the relationship between two or more waves. Let us assume that the waves originate in a light source and phase δ contains information on how the wave was formed. Light waves are created by emission processes and there is an emission procedure for every photon or light wave. The emission procedures are distributed statistically according to the type of the light source. Thus, the frequency or phase δ is also distributed statistically. If the emission procedures are coupled to each other, as is the case with lasers, and all photons or waves have the same frequency or wavelength such light is termed as coherent (holding itself together).

If, however, phase δ is randomly distributed, then this light is incoherent. This is the case with thermal light sources, e.g. light bulbs. According to Fig. 6 the wave 2 has a phase shift of δ as opposed to the wave 1. If we produced two such waves (this is exactly what the Michelson interferometer does), we expect a third wave through the principle of superimposition, which is formed by the superimposition or interference of the two basic waves. We will find out how this wave looks like by simply adding both basic waves:

Wave 1 $$\vec{E}_1 = \left(E_{Y,}E_Z\right) \cdot \sin\left(k \cdot x + \omega \cdot t + \delta\right)$$

Wave 2 $$\vec{E}_2(Y,Z) = \left(E_{Y,}E_Z\right) \cdot \sin\left(k \cdot x + \omega \cdot t\right)$$

Wave(1,2) $$\vec{E}_3 = \vec{E}_1 + \vec{E}_2$$

A large number of waves with different frequencies ω or wavelengths λ and phases δ result in such a confusing mixture and it makes no practical sense to carry out superimposition or interference experiments with such light. Therefore, light sources which emit light within a narrow emission

Theory

spectrum with a phase as constant as possible are selected. Lasers are an example of such light sources. The other extreme is the use light sources of extremely broad spectral emission, like the whit light interferometry.
But when Michelson carried out his experiments around 1870 he had no lasers. He used instead the red atomic emission line of a cadmium lamp whose emission bandwidth has a coherence length of only 20 cm requiring sophisticated experimental arrangements.

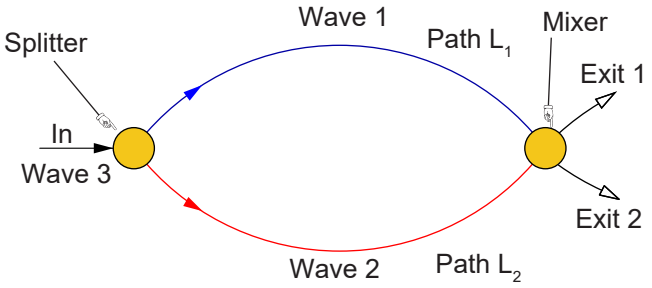

Fig. 7: Generalized treatment of interference

We will discuss basic devices to superimpose light waves like the Michelson interferometer. A generalized approach is shown in Fig. 7. Each interferometer uses a light source (Wave 3), which radiation is split into two portions of equal intensity. An ideal splitter would not affect neither the wavelength nor the phase of the created waves. Wave 1 and wave 2 are travelling along individual paths and are combined in the mixer. It should be noted, that each interferometer has at least two exit paths, which is required to fulfil the energy conservation. As we will see later that in case of a destructive interference at exit 1 the energy is not destroyed, but it leaves the interferometer at exit 2.

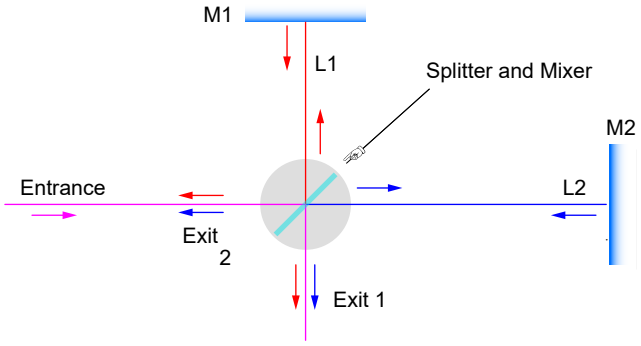

Fig. 8: The famous Michelson interferometer

Such an arrangement, shown in Fig. 8, is the famous Michelson interferometer. In this setup the splitter and mixer are identical.

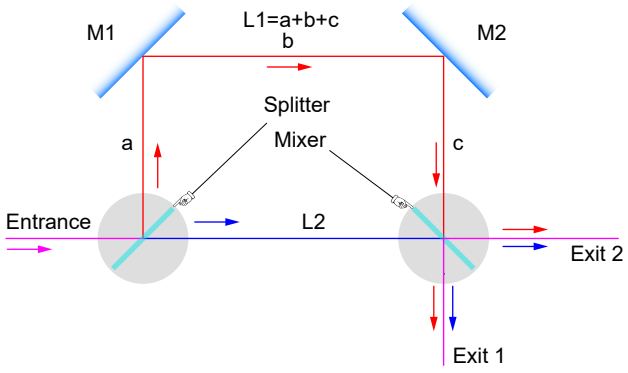

Fig. 9: Mach Zehnder interferometer with separate splitter and mixer

Both interferometers belong to the class of two-beam interferometer. A famous example of multi-beam interferometer is the Fabry Perot interferometer. However, we will not treat it here.
Since in practical interferometer the superimposing beams travel collinear to one another we can simplify the equations and writing now:

Wave 1 $$E_1 = E_{01} \cdot \sin\left(k \cdot L_1 + \omega \cdot t\right)$$

Wave 2 $$E_2 = E_{02} \cdot \sin\left(k \cdot L_2 + \omega \cdot t\right)$$

Wave 3 $$E_3 = E_1 + E_2$$

Note, there is no phase shift between wave 1 and wave 2 because they are created from wave 3 and the splitter does not create an extra phase shift.

$$E_3 = E_{01} \cdot \sin\left(k \cdot L_1 + \omega \cdot t\right) + E_{02} \cdot \sin\left(k \cdot L_2 + \omega \cdot t\right)$$

Let us install a screen or photodetector at exit 1 to observe the resulting intensities. The human eye as well as photodetector cannot register pure electric fields, but can only register the light intensity I which is connected to the field strength:

$$I = E^2 = \left(E_1 + E_2\right)^2$$

$$I = \left(E_1 \cdot \sin\left(k \cdot L_1 + \omega \cdot t\right) + E_2 \cdot \sin\left(k \cdot L_2 + \omega \cdot t\right)\right)^2$$

$$I = E_1^2 \cdot \sin^2\left(kL_1 + \omega t\right) + 2E_1E_2 \cdot \sin\left(kL_1 + \omega t\right) \cdot \sin\left(kL_2 + \omega t\right) + E_2^2 \cdot \sin^2\left(kL_2 + \omega t\right)$$

By using the well known addition theorem

$$2 \cdot \sin\alpha \cdot \sin\beta = \cos\left(\alpha - \beta\right) + \cos\left(\alpha + \beta\right)$$

we get:

$$I = E_1^2 \cdot \sin^2\left(kL_1 + \omega t\right) + E_1E_2 \cos\left(k\left(L_1 - L_2\right)\right) + E_1E_2 \cos\left(k\left(L_1 + L_2\right) + 2\omega t\right) + E_2^2 \cdot \sin^2\left(kL_2 + \omega t\right)$$

The fastest photodetector nowadays can follow frequencies of up to approx. 1×10^9 Hz (1 GHZ). This is why a detector, and even more so, our eyes can only perceive slow varying average values. The $\sin^2$ terms oscillate between 0 and 1; its temporal average value is therefore 1/2. The cosine term oscillates between -1 and +1, the average value is zero, simplifying the equation to:

$$I = \frac{1}{2}E_1^2 + \frac{1}{2}E_2^2 + E_1E_2 \cos\left(k \cdot \Delta L\right) \qquad \textbf{(2)}$$

with $\Delta L = L_1 - L_2$.
Obviously the intensity I becomes maximal when the cosine value becomes 1. This is always the case when its argument is zero or a multiple of 2π. The intensity I becomes minimal when the value of the cosine is –1 which is the case when its

argument is a multiple of π.

$$I_{max} = \frac{1}{2}E_1^2 + \frac{1}{2}E_2^2 + E_1E_2 = \frac{1}{2}(E_1 + E_2)^2$$

$$I_{min} = \frac{1}{2}E_1^2 + \frac{1}{2}E_2^2 - E_1E_2 = \frac{1}{2}(E_1 - E_2)^2$$

Let us recall that the wave number k is defined as:

$$k = \frac{2\pi}{\lambda}$$

and that it is constant for a given wavelength. Thus, the light intensity *I* of eq. (2) depends only on the path difference $\Delta L = L_1 - L_2$. If the paths having the same length, both partial waves superimpose constructively and the light intensity becomes maximal. If the path difference however, is just λ /2 then the wave number k becomes:

$$k \cdot \Delta L = \frac{2\pi}{\lambda} \cdot \frac{\lambda}{2} = \pi ,$$

and the value of the cosine is -1 and the light intensity *I* becomes minimal. If E_1 and E_2 have the same intensity, the light intensity *I* even becomes zero, both waves superimpose destructively.

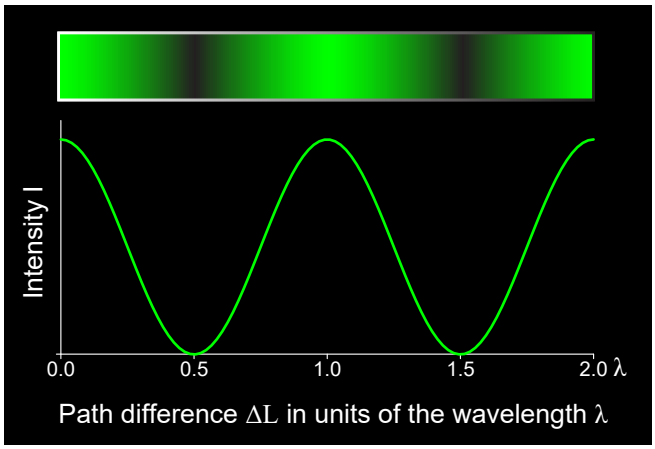

Fig. 10: Interferogram as per eq. (2)

Observing for instance a number of *N* dark / bright transitions, a length difference of $\Delta L = N\cdot\lambda/2$ occurred. Keeping in mind, that the wavelength used in our experiments is 532 nm, a light to a dark transition already occurs with a phase shift by only

λ/2=266 nm = 0.000000266 mm (!).

Thus, this type of interferometer is a highly precise apparatus for measuring length.

Up to now we assumed that the wavelength λ has a singular value, which is neither theoretical nor practical possible. Theoretically it would violate the Heisenberg's principle and thus in practice no light source exists with a sharp emission line of zero line width.

We will shortly shine some light on what will happen to the results when the light source has a spectral distribution.

In this case the intensity I_0 is a now a function of ω:

$$I_0 \rightarrow \hat{I}(\omega) = \hat{I} \cdot \rho(\omega) \cdot \partial\omega$$

Where ρ(ω) is the line shape of emission line.

So, we must integrate over all ω:

$$I = \int_{-\infty}^{+\infty} \left\{ \hat{I} \cdot \rho(\omega) + \hat{I} \cdot \rho(\omega) \cdot \cos(\omega / c \cdot \Delta L) \right\} \cdot \partial\omega$$

and obtain for the interferogram

$$I = I_0 + \int_{-\infty}^{+\infty} \hat{I} \cdot \rho(\omega) \cdot \cos(\omega / c \cdot \Delta L) \cdot \partial\omega \qquad \textbf{(3)}$$

We can obtain the contrast or the visibility of the interference from the extreme values of (3):

$$V(\Delta L) = \frac{I_{max} - I_{min}}{I_{max} + I_{min}}$$

Thus the contrast function V, which is still dependent on ΔL after the integration, is the envelope of the interferogram I(ΔL). According to the form the emission line takes, or how the function ρ(ω) is made up, we can obtain the contrast of the function of the path difference ΔL and the corresponding contrast function V(ΔL) by using the above integration. The emission line of the laser, which we will use in the later experiment, can be described using a Gaussian function with a bandwidth Δω. The integral according to (3) can be calculated in this way and is given in detail in [Max Born, Optik, Springer Verlag, Berlin Heidelberg New York 1981] and the contrast function is shown in the following diagram.

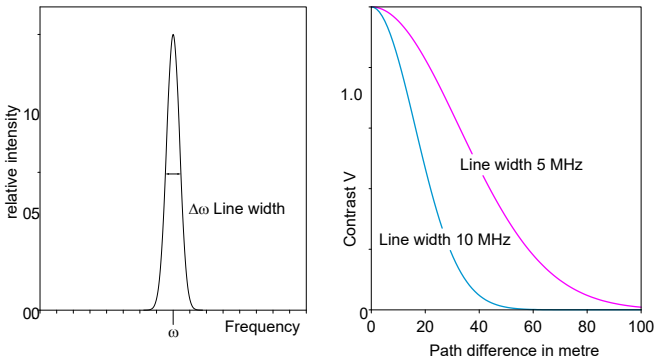

Fig. 11: Contrast V as a function of the path difference of a light source with an emission bandwidth of 5 or 10 MHz (Laser).

The diagram on the right hand side of Fig. 11 shows the contrast function. It shows that the contrast in a Gaussian distribution curve gradually drops as the path difference ΔL between both interfering waves increases. Theoretically, if the path difference is infinitely long, the contrast will eventually be zero. We notice that for a light source emitting a beam with a spectral width Δω of 5 MHz has a coherence length of about 100 metre. However, a light source with a broad emission bandwidth has a very short coherence of a few micrometer only. It appears, that interferometer operated with such light sources make no sense! But, if we recall (3):

$$I = \frac{1}{2}E_1^2 + \frac{1}{2}E_2^2 + E_1E_2\cos(k \cdot \Delta L)$$

The requirement for the cos() to be zero can also be fulfilled when ΔL is very close or even 0, that means that L_1 equals L_2. In this case interference appears independent of the wavelength λ.

Theory

3.0 Description of the components

3.1 Michelson Laser Interferometer

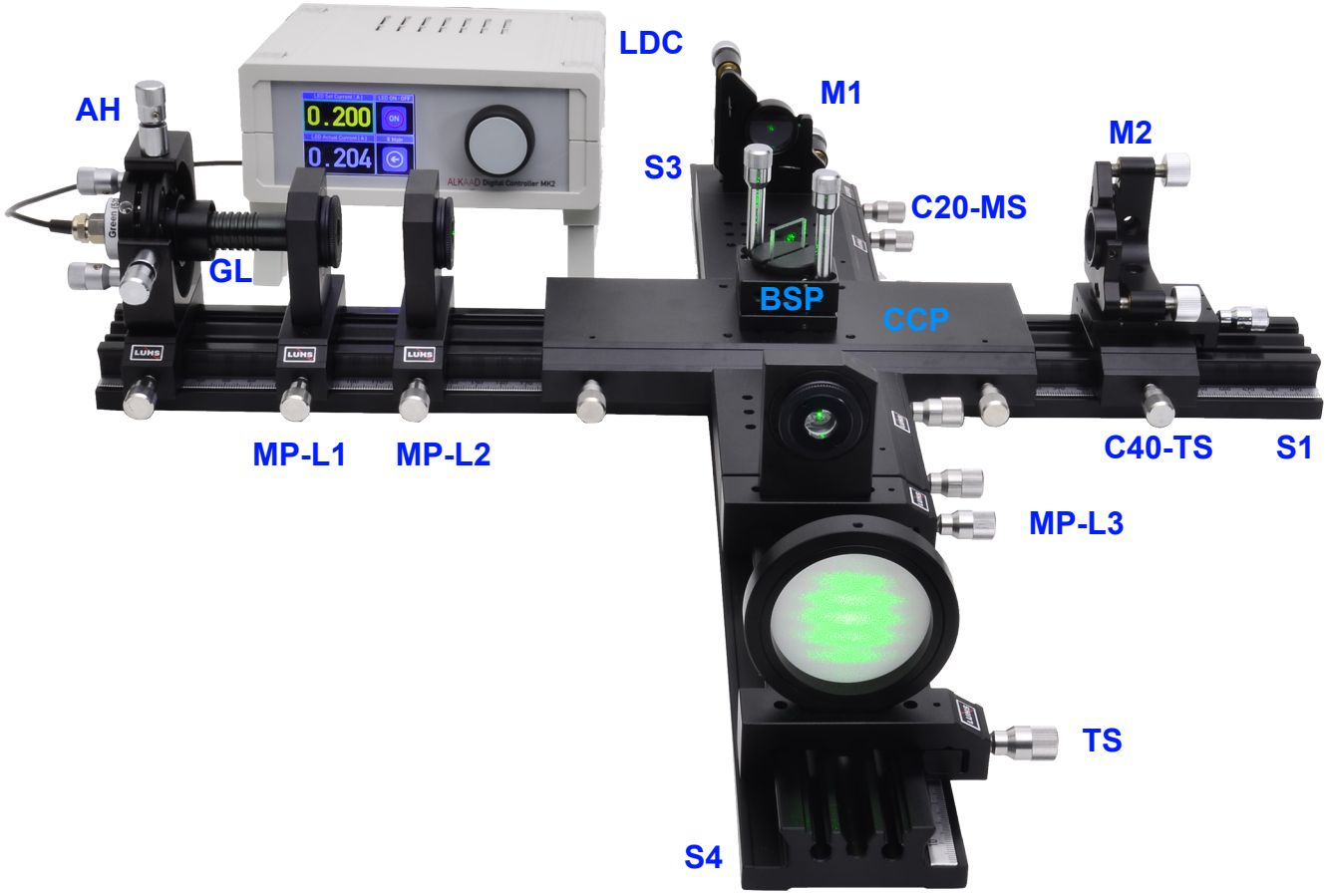

AH Adjustment Holder

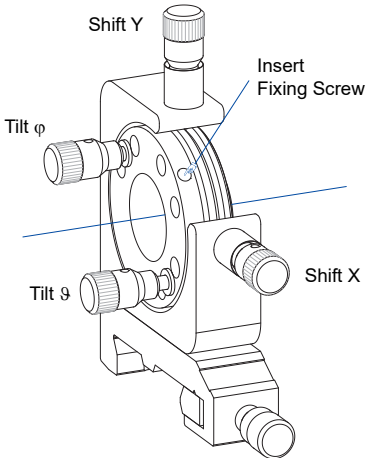

Fig. 12: MM-0420 Four axes kinematic mount on carrier MG20

This frequently needed component is ideal for the fine adjustment of lenses, microscope objectives, diode laser, etc. with respect to the optical axis of the rail set-up. The displacement area is 5x5 mm and 10x10 degrees respectively. Different mounts can be attached to the adjustment holder. This model provides a holder for 25 mm cylindrical components. The component is inserted into the adjustment holder and is kept in position by a grub screw with a nylon tip. Four precise fine pitch screws of repetitious accuracy allow the translational (X; Y) and azimuthal (υ; φ) adjustment.

GL Green Laser

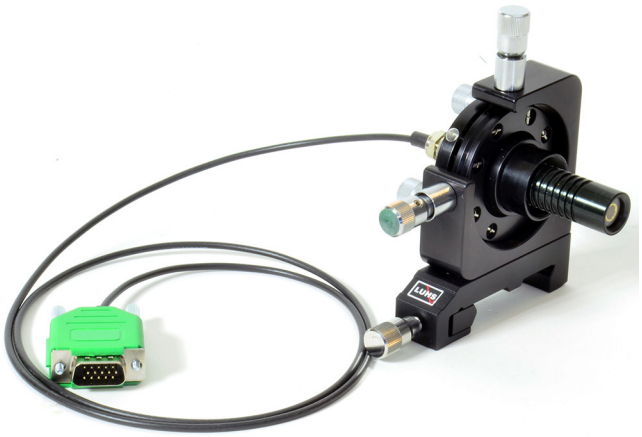

Fig. 13: LQ-0020 Green (532 nm) DPSSL in ø25 housing inserted into the 4 axes kinematic mount

A green (532 nm) emitting DPSSL (Diode Pumped Solid State Laser) is integrated into a C25 housing and is operated with the “DC-0020 LED Controller”. The output power is < 5 mW. The diode laser is connected via a 15 pin SubD HD connector to the controller MK2. Inside the connector an EEPROM contains the data of the laser diode and when connected to the controller, these data are read and displayed by the controller.

MP-Lx Mounting Plate with Lens x

Fig. 14: MM-0020 Mounting plates C25 and C30 on carrier MG20

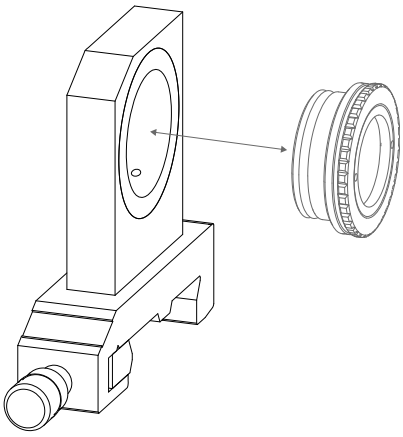

This frequently used component is ideal to accommodate parts with a diameter of 30 or 25 mm where it is kept in position by three spring loaded steel balls. Especially C25 or C30 mounts having a click groove are firmly pulled into the mounting plate due to the smart chosen geometry. The mounting plate is mounted to a 20 mm wide carrier.
The f=40 mm achromat is used to collimate the emission of the white light LED. The combination of the f=-15 mm and f=60 mm forming an adjustable beam expander with expansion factor of 4. The single lens of f=-15 is used as imaging lens for the interference patterns.

S1, 2 (500 mm),S3 (200 mm), S4 (300 mm) Optical rails

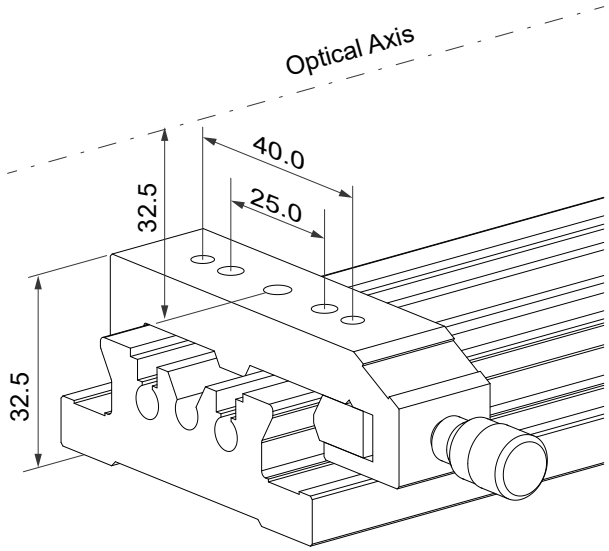

Fig. 15: Rail and carrier system

The rail and carrier system provides a high degree of integral structural stiffness and accuracy. Due to this structure it is a further development optimised for daily laboratory use. The optical height of the optical axis is chosen to be 65 mm above the table surface. The optical height of 32.5 mm above the carrier surface is compatible with all other systems like from MEOS, LUHS, MICOS, OWIS and LD Didactic. Consequently a high degree of system compatibility is achieved.
A set of 2 x 500 mm, 300 mm and 200 mm are provided for various set-up combinations of a Michelson or Mach Zehnder Interferometer

M1 Mirror in Adjustment holder on Carrier

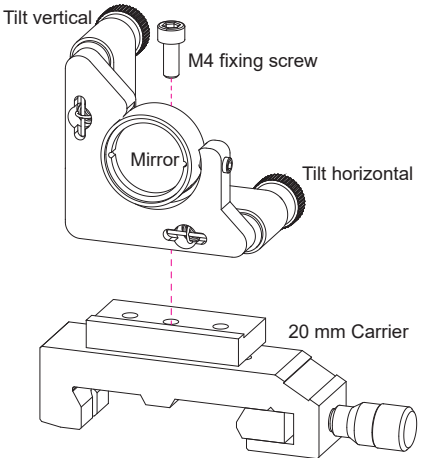

Fig. 16: MM-0440 Kinematic mount ø25.4 mm on MG20, left

The adjustment holder (AH) comprises two high precision fine pitch screws. The upper screw is used to tilt the moveable plate vertically and the lower one to tilt it horizontally. By means of an M4 screw the adjustment holder is attached to the 20 mm carrier.

M2 Mirror in Adjustment holder on translation stage and carrier 40 mm

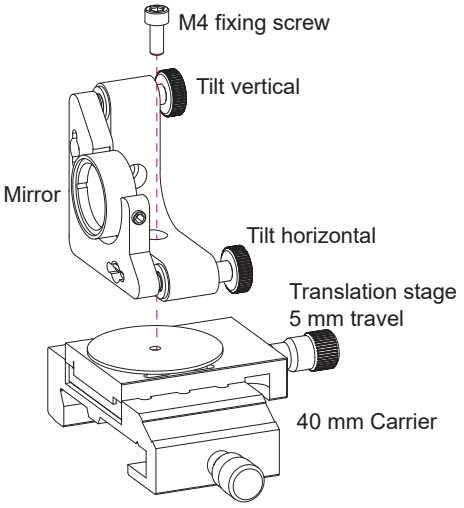

Fig. 17: MM-0444 Kinematic mount 1", translation stage on MG65

By means of an M4 screw the adjustment holder is attached to the translation stage with a travel range of 5 mm The set screw has a pitch of 250 µm, which is two times finer than industrial micrometer screws. One turn of the screw shifts the mirror by 250 µm.

BSP Adjustable Beam splitter Unit

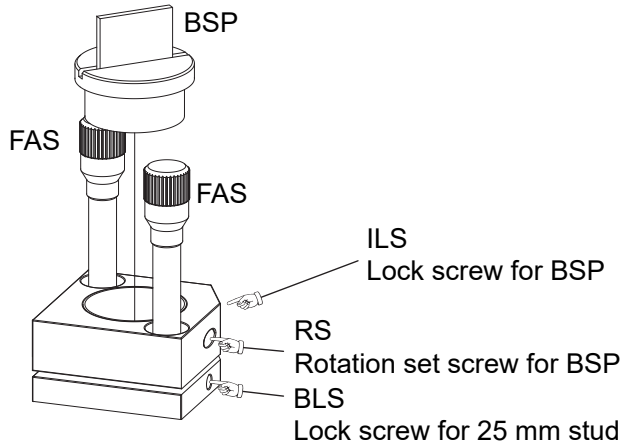

Fig. 18: OM-0010 Adjustable beam splitter

The beam splitting plate (BSP) is mounted into a holder and divides the incoming beam at a ratio of 1:1. The mount is inserted into the adjustment holder and fixed by the lock screw (ILS) and can be turned around its vertically axis by turning the screw (RS). For this purpose an Allan key screwdriver is provided. By means of the two fine adjustment screws (FAS) the beam splitting plate can be tilted. The adjustment holder is fixed by means of the lock screw (BLS) to the crossed carrier.

CCP Carrier Cross Piece

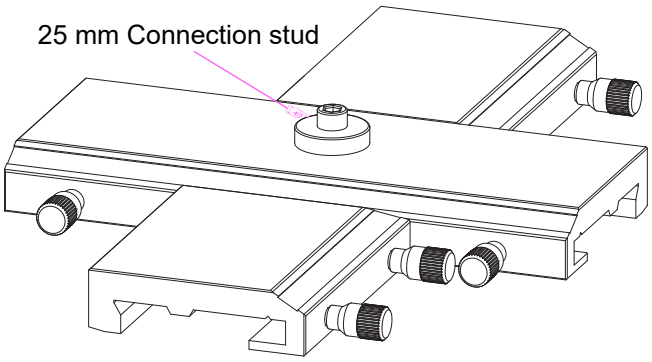

Fig. 19: MP-0065 Carrier cross piece MG-65

This component is used to combine a long middle rails and two shorter ones to a cross structure. In its centre a 25 mm stud is fixed to which the adjustable beam splitter

TS Translucent Screen

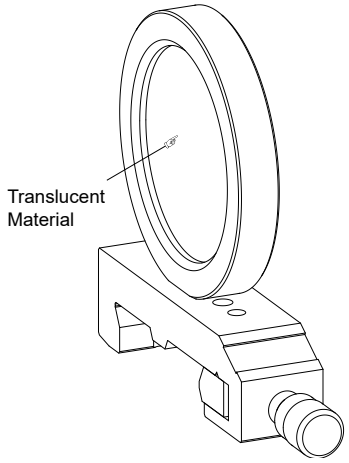

Fig. 20: MM-0110 Translucent screen on carrier MG20

In a round holder a sheet of translucent paper is fixed with a retaining ring. This component is useful to image and visualize optical rays. Furthermore, the translucence allows the convenient photographic recording from the opposite side with digital cameras for a quick picture for the students measurement report.

LDC LED Controller

This microprocessor operated device contains an LED current controller and optional a photodiode amplifier. A touch panel display allows in conjunction with the digital knob the selection and setting of the parameters for the attached LED or photodiode. The controller reads the operation values of the connected LED or laser from the EEPROM located inside its connector. The device comes with a 230 VAC / 12 VDC wall plug power supply. The device can be controlled and the data read by an external computer via the USB bus.

Fig. 21: The rear of the MK2 controller

The controller is operated by 12 VDC via the provided wall plug power supply. The LED or laser are connected via the 15 pin SubD connector labelled “LED/LD”. When the LED or laser is operated in modulated mode, the reference modulator signal is available at the “MODULATOR” BNC connector.

When the external 12 V is applied and switched on, the controller starts displaying the screen as shown in the figure above.

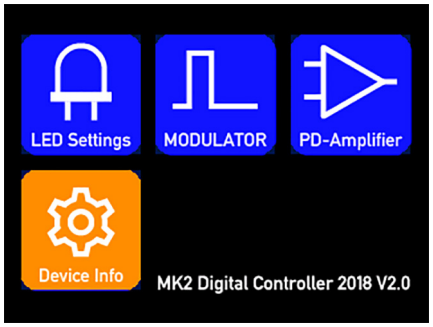

The upcoming interactive screen appears with the selection of 4 buttons:

1. LED/Laser current settings
2. Modulation of the LED/laser
3. Photodiode Amplifier (only as option)
4. Device and LED/laser information
5.

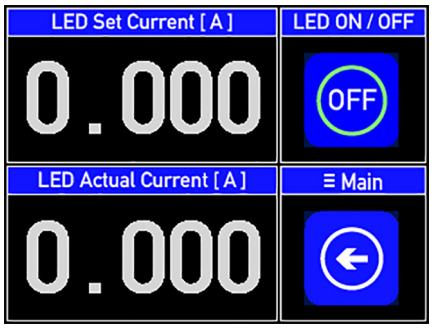

The current settings screen shows the set current as well as the actual current. With the LD ON/OFF touch button the laser is switched on or off. The ≡Main touch button switches back to the main page.

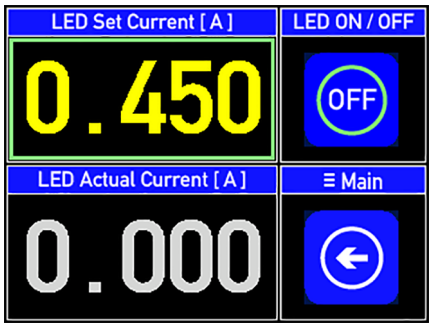

By touching the “LED Set Current” display field it is highlighted. By turning now the knob, the value of the injection current can be set and is immediately applied, provided the LED ON/OFF touch button is activated.

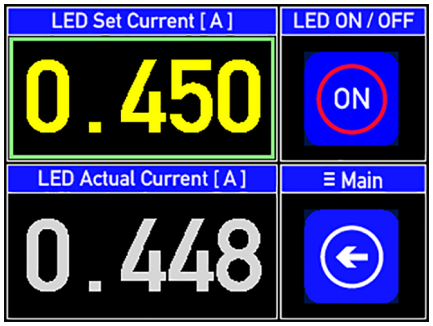

Touching the LED ON/OFF button switches the LED ON or OFF. When switched ON, the actual current is displayed in addition.

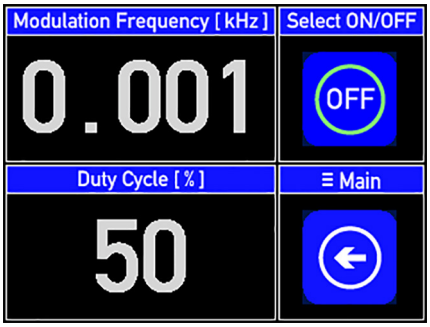

The LED or laser can be switched periodically on and off. This is for a couple of experiments of interest.

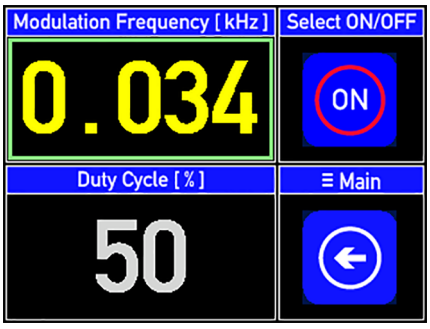

By tapping the display of the modulation frequency the entry is activated. Turning the settings knob will set the desired frequency value. The modulation becomes active, when the Modulator ON/OFF button is tapped.

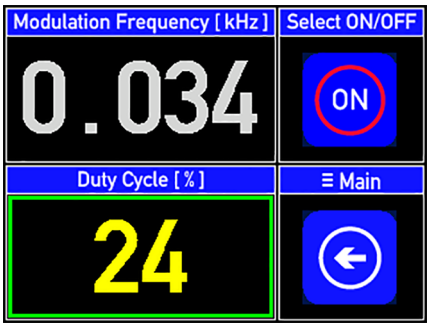

For some experiments it is important to keep the thermal load on the optically pumped object as low as possible or to simulate a flash lamp like pumping. For this reason the duty cycle of the injection current modulation can be changed in a range of 1...100 %. A duty cycle of 50% means that the OFF and ON period has the same length. The set duty cycle is applied instantly to the injection current controller.

This screen appears only, when no LED or laser is connect to the device

3.2 Michelson White Light Interferometer

White Light LED

Fig. 22: LQ-0200 White LED in ø 25 Housing

A white light LED is built into a round housing (C25). The LED is connected via a 15 pin SubD HD connector to the controller MK1. Inside the connector an EPROM contains the data of the LED and when connected to the controller, these data are read and displayed by the controller.

Crosshair Reticles in C25 mount

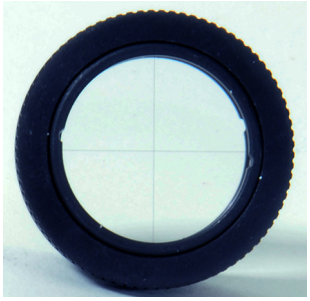

Crosshair (crossline) reticles are used to superimpose a reference pattern on an object being imaged. The crosshairs, formed from lines that are 10 µm wide, span the entire diameter of the optic. Made by plating chrome onto one side of a 1.5 mm thick UV fused silica substrate, these optics provide greater than 90% transmission in the 200 - 1200 nm spectral range.

Precision Vernier

For the precise measurement of the distance of mirror M1 and M2 such a precision vernier is provided.

3.3 White Light Interferometer with Audi Fringe Detection

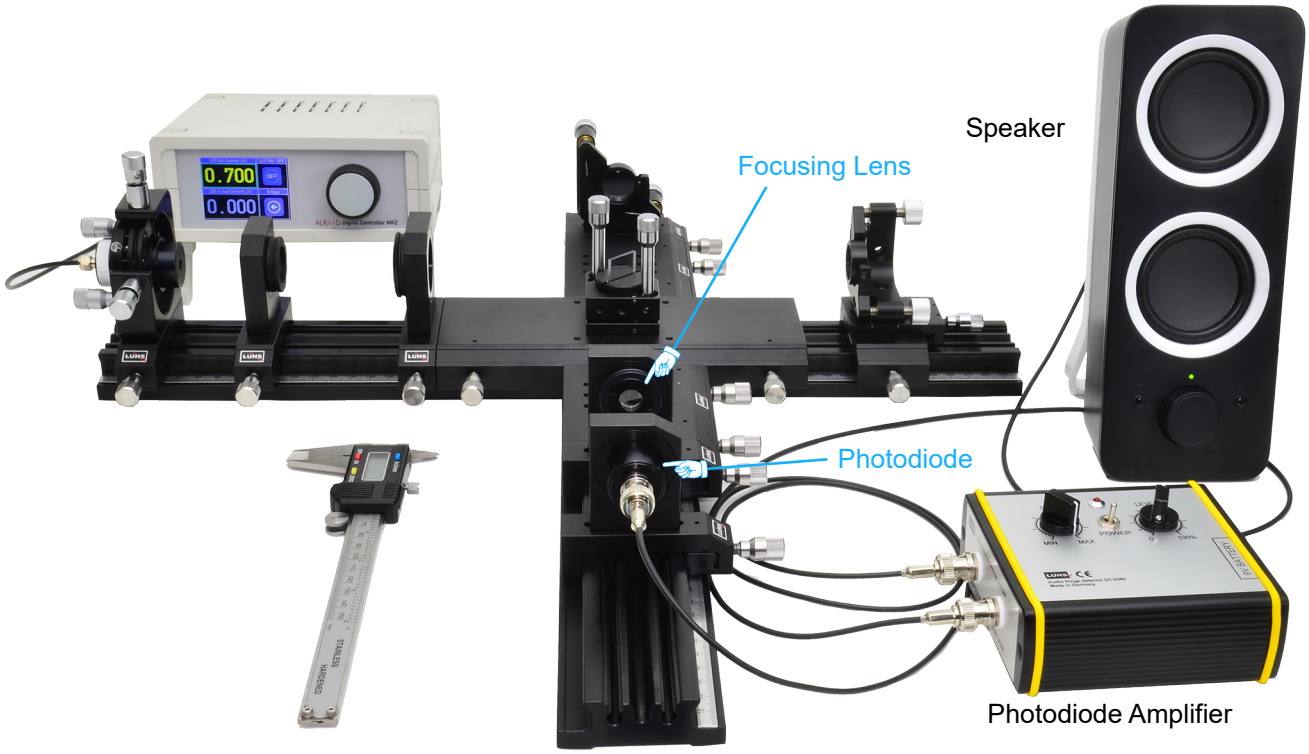

DC-0260 Audio fringe detector

Fig. 23: DC-0260 Audio fringe detector

This device is an audio amplifier with an input designed for a photodiode which is connected via a BNC panel jack. Changes of the light intensity falling onto the detector will be converted into an audible sound. An external active speaker is used to listen to the light intensity changes. This detector is very useful for white light interferometer to detect the appearance of fringes.

Active Speaker

Photodiode

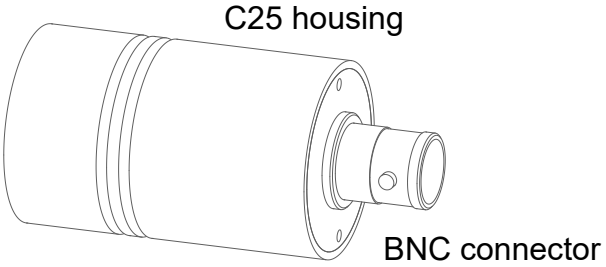

Fig. 24: DC-0120 Si-PIN Photodetector, BPX61

A Si PIN photodiode is integrated into a 25 mm housing with two click grooves. A BNC connector is attached to connect the module to other devices. The photodetector module is placed into the C25 mounting plate where it is kept in position by three spring loaded steel balls.

Parameter	Symbol	Value	Unit
Rise and fall time of the photo current at: R_L=50Ω; V_R=5 V; λ=850 nm and I_p=800 µA	t_r, t_f	20	ns
Capacitance at V_R = 0, f = 1 MHz	C0	72	pF
Wavelength of max. sensitivity	λ_{Smax}	850	nm
Spectral sensitivity S 10% of S_{max}	λ	1100	nm
Dimensions of radiant sensitive area	L × W	7	mm^2
Spectral sensitivity, λ = 850 nm	S(λ)	0.62	A/W

Table 1: Parameter of the photodiode BPX61

3.4 Mach Zehnder Interferometer

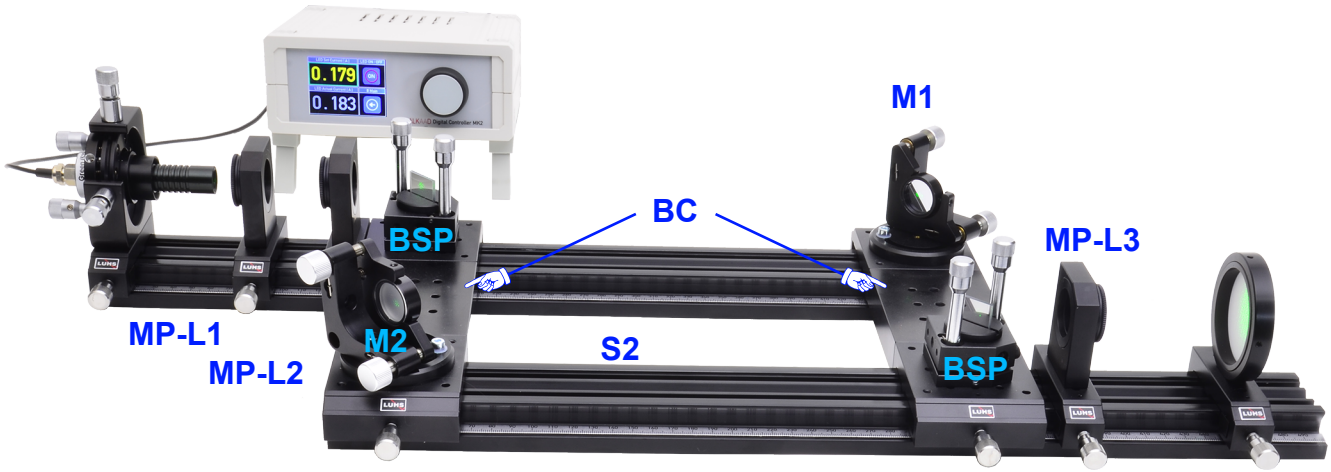

BC Bridge connector

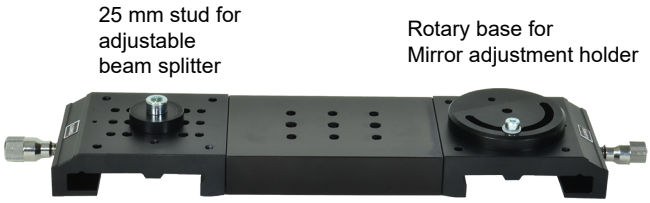

Fig. 25: MP-0082 Bridge connector for two rails plus riser plate

A pair of such bridge connectors are used to combine two 500 mm rails to obtain the structure of the famous Mach Zehnder interferometer. From the Michelson setup the adjustable beam splitter as well as the two mirror adjustment holders are transferred onto each bride.

3.5 Mach Zehnder Interferometer with Vacuum Cell

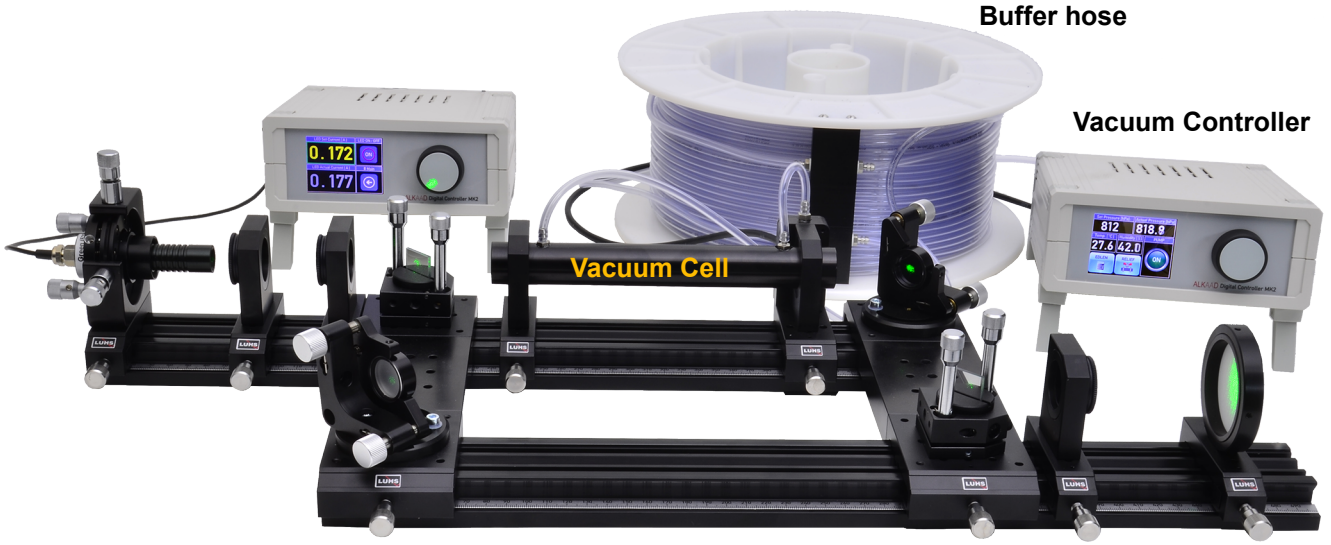

Vacuum Cell

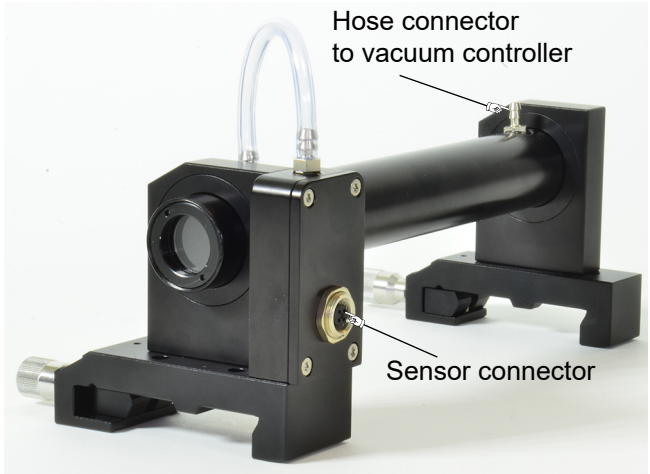

Fig. 26: OM-0820 Gas cuvette assembly

A 25 mm housing with a length of 200 mm is vacuum proof sealed by two optical glass windows. The cuvette is held by two mounting plates. The cuvette has two hose connections, one is connected to the high precision sensor and the other one is connected to the “DC-0110 Vacuum Controller”. The sensor measures the pressure inside the cell, the temperatures as well the relative humidity. The sensor is connected via a 4 pin connector to the vacuum controller.

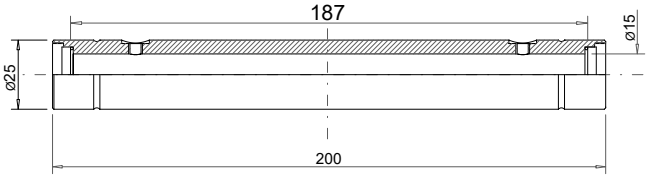

Fig. 27: Dimension of the vacuum cell

Buffer Hose

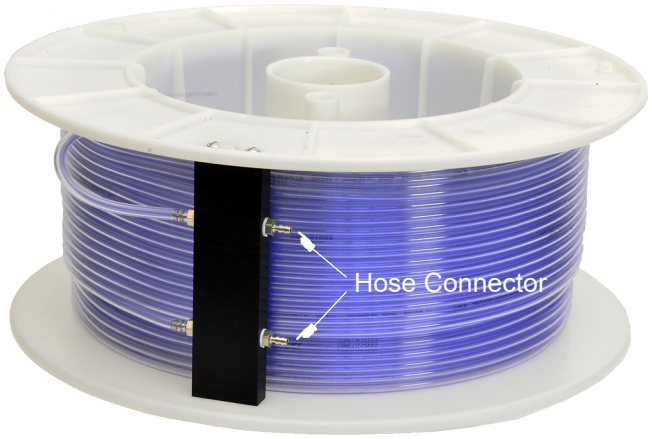

The task of the experiment is to count the fringes while the pressure inside the cell is reduced by a known amount. To reduce the speed of the fringe changes, the volume of the cell is increased by this 100 m long hose. It has an inner diameter of 4 mm thus adding 1.3 litre extra to the volume of 33 cm^3 of the cell

Fig. 28: Alignment Iris in mounting plate with 4 mm fixing pins

The adjustable iris is mounted into a C25 mount and has a minimum opening of 1 mm and the maximum opening is 14 mm. It can be either mounted into the above shown mounting plate or into a mounting plate attached to a carrier.

DC-0110 Vacuum Controller

Fig. 29: DC-0110 Vacuum Controller

The DC-0110 is a microprocessor controlled vacuum pump. A miniaturised membrane pump creates a vacuum down to 350 hPa. On the rear the controller provides a 4 mm hose connector (VAC PUMP) and the 4 pin connector for the sensor (SENSOR). For the operation a 12VDC wall plug power supply is provided. A touch screen and digital rotary knob allows the control and entering of the set pressure in a range of 350 hPa to local air pressure.

After switching on, the controller shows the start screen. With a touch the next screen appears.

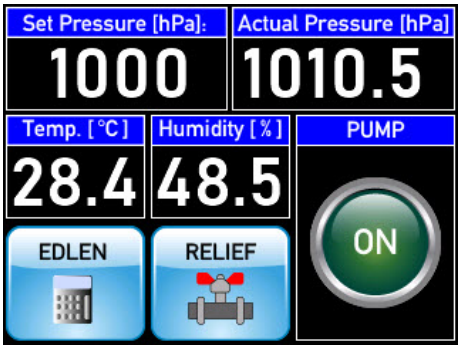

This screen allows the functions as described below.

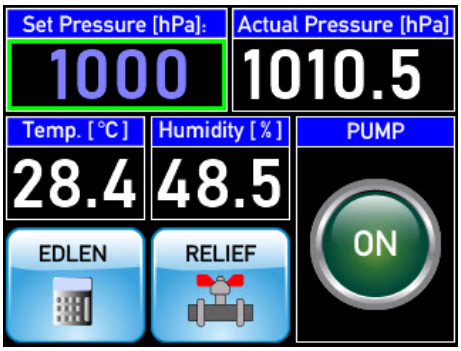

Touching into the Set Pressure display filed activates this and by turning the digital knob the desired pressure is selected.

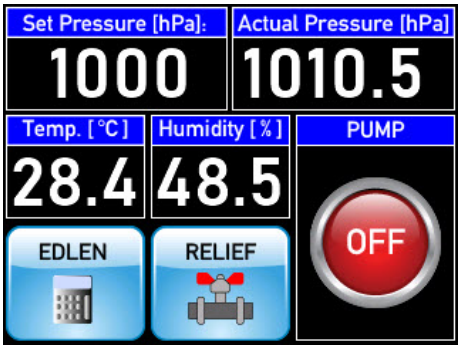

Touching the PUMP button starts or stops the vacuum pump. The pump is running until the actual pressure reaches the set pressure in certain limits. It will not exactly, however,

it is important to know the reached value of the pressure. Simultaneously to the pressure the temperature as well as humidity are measured and displayed. Touching the EDLEN button opens the page with calculations for the index of refraction inside the cell based on the measured values.

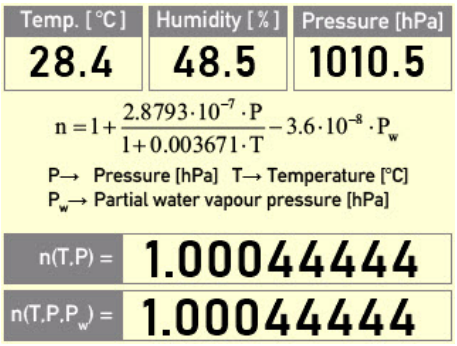

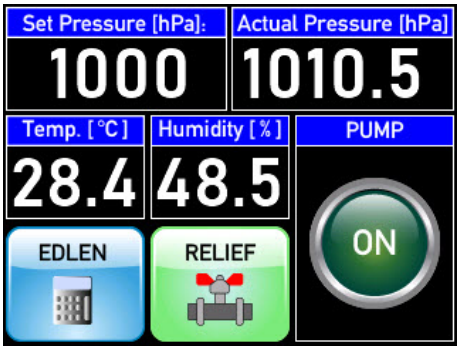

By pressing and holding the RELIEF button opens the valve to the environment and the pressure inside the cell reaches the air pressure.

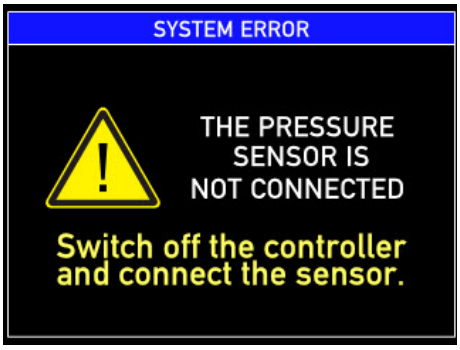

In case the sensor is not connected to the controller this warning screen comes up.

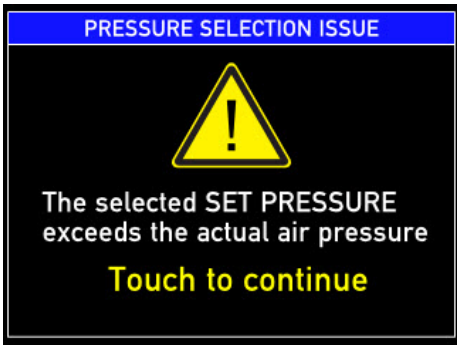

In case the selected pressure is higher than the environmental air pressure this screen shows the warning.

4.0 Set-up and Measurements

4.1 Michelson Laser Interferometer

Within this section the step by step procedure to setup the Michelson interferometer with a laser as light source is explained.

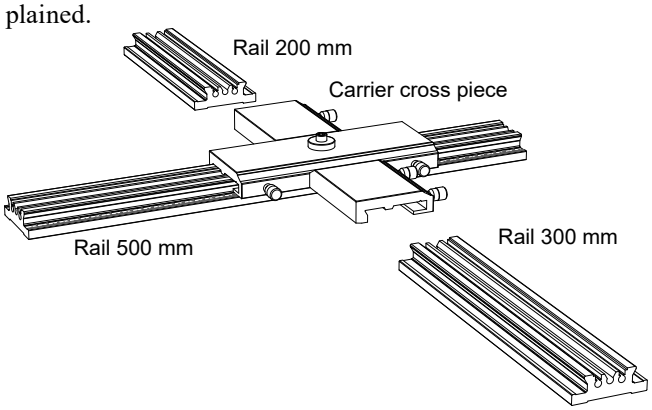

The 500 mm long rail is inserted into the carrier cross piece.

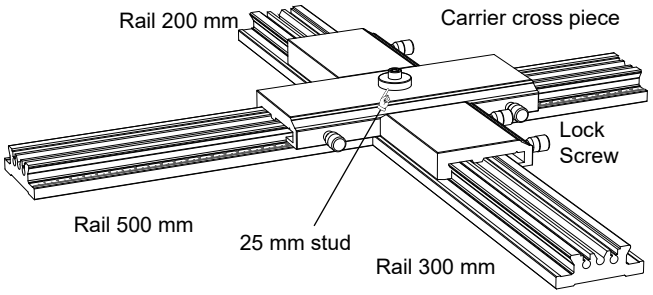

Subsequently the 200 mm and the 300 mm rails are attached such, that they are butt against the middle piece. All lock screws are tightened.

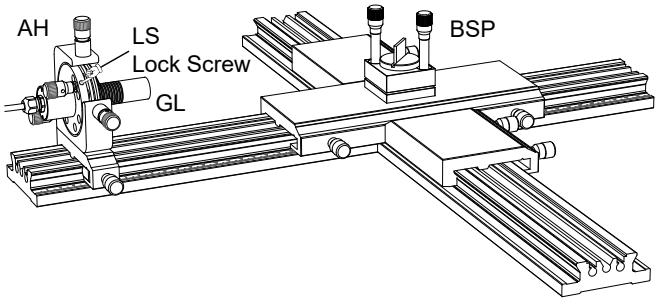

Within this step the adjustable beam splitter (BSP) is attached and fixed to the 25 mm stud of the carrier cross piece. The green laser (GL) is inserted into the adjustment holder (AH) and locked by the lock screw (LS).

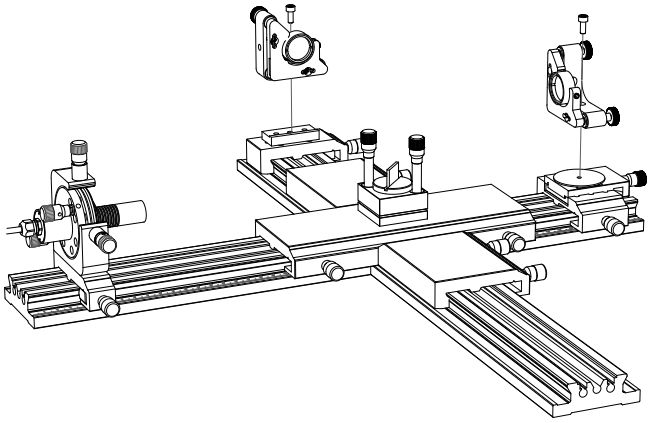

The mirror adjustment holder are attached to their respective carrier with the M4 screws.

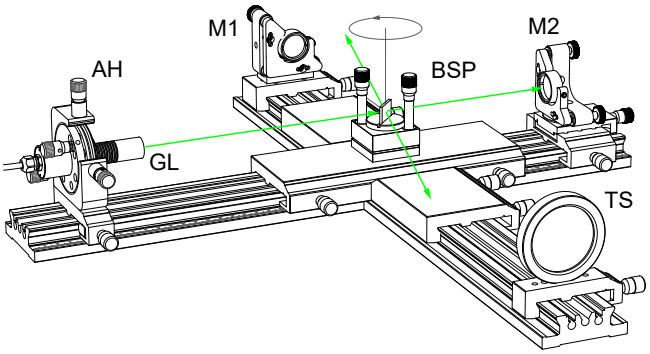

The green laser is set to low power and switched on. The green laser beam is aligned with the adjustment holder (AH) such, that the beam (B) hits the centre of mirror M2. Reflections at the beam splitter plate occur. To observe and align the created beams, the translucent screen (TS) is attached to the rail. It is recommended to orientate the beam splitter plate's reflecting side facing to mirror M1.

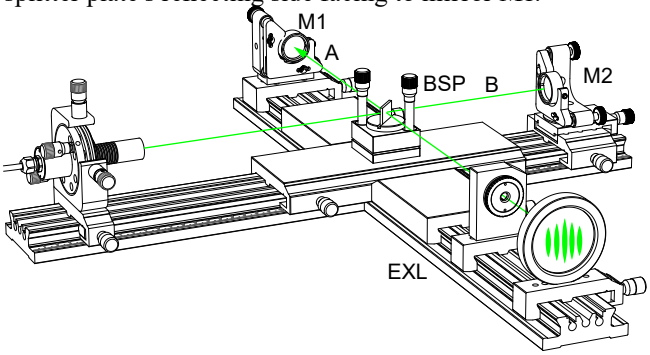

In the next step, the beam splitter plate is aligned in order to direct the reflected beam (A) to the centre of M1. Align the mirror M2 so, that the reflected beam B hits the centre of the translucent screen (do not use the expansion lens at this moment). Now mirror M1 is aligned such, that the reflected beam (A) falls into the same spot on the screen as (B). Now it is time to insert the expansion lens and first interference should be visible. The gentle fine tuning of all components results in a clear and crisp interference pattern. It may happen, that the contrast of the fringes comes out not as expected. The reason might be, that the laser oscillates instead of single mode in two or more modes. In such a case change the injection current of the laser and it will jump back to single mode.

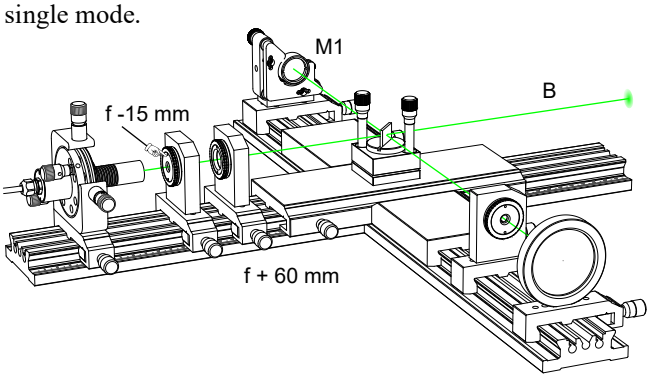

Fig. 30: Using the beam expander to create circular interference fringes.

Remove the mirror M2 and let the beam B travel freely (take care about laser safety) against a wall in a distance of 2 or more metre. Insert the lenses as shown in Fig. 30. Both lens-

es form a telescope which expands the beam diameter by a factor of 4, provided the distance of the lenses to each other is set correctly. This is the case, when the beam behind the telescope has an almost constant beam diameter all over the travelled path to the wall. Now we add the mirror M2 again to the setup. After slight alignment we should observe interference parallel interference fringes, since due to the perfect alignment of the beam expansion lenses we still have plane waves.

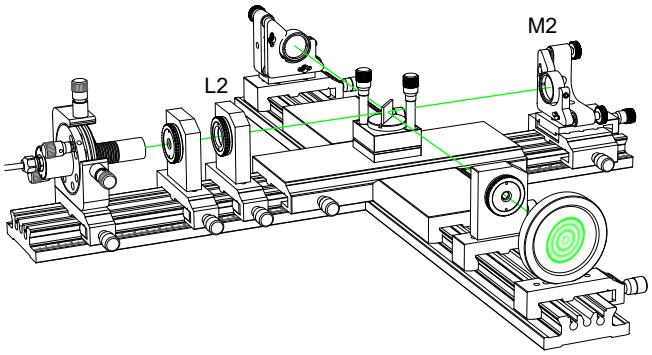

If we now moving the lens L2 slightly away from the ideal position, the laser beam becomes divergent resulting in a circular interference structure due to the curved wave fronts of the divergent laser beams.

4.2 White Light Interferometer

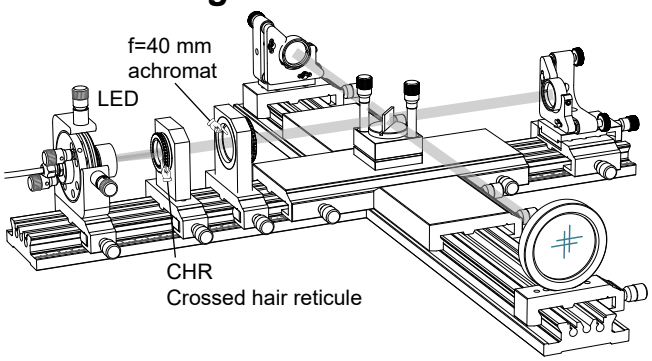

Fig. 31: White light interferometer with auto-collimation technique

In the white light setup the green laser is replaced by a LED which emits a mixture of red, green and blue emission appearing as white light to the human eye. The individual emission profile however are fairly broad, see Fig. 32.

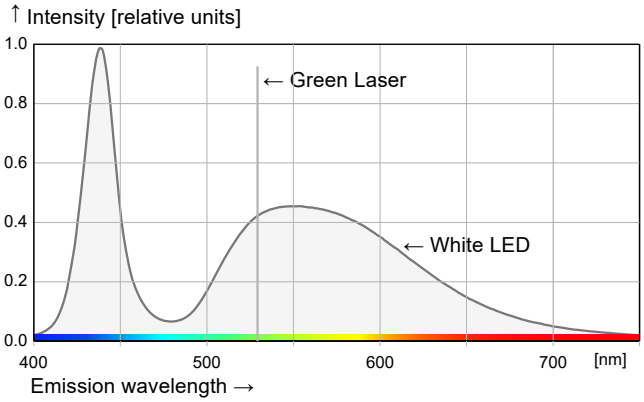

Fig. 32: Spectrum of a white light LED

In general a white light interferometer is very hard to align, since two sensitive parameters needs to be monitored. Firstly the perfect alignment of the mirror M1 and M2 to each other and secondly the distance between both mirrors.

To overcome the difficulty of the mirror alignment we make use of the auto-collimation technique. A cross hair reticule (CHR) is placed in front of the white LED. The achromatic lens transfers the images of the crossed hair onto the translucent screen and that for both mirrors M1 and M2. If the mirrors are not correctly aligned, two crossed hair images appear on the translucent screen (see Fig. 31). If both crosses overlap, the alignment is perfect. The next crucial parameter is the distance of both mirror. More precise, the optical path lengths L1 and L2 must be identical within an accuracy of the coherence length Lc of the light source:

$$L_c = \frac{c}{\Delta\nu} = \frac{\lambda_1 \cdot \lambda_2}{\lambda_2 - \lambda_1} = \frac{\lambda_1 \cdot (\lambda_1 + \Delta\lambda)}{\Delta\lambda}$$

If, for instance the emission bandwidth λ_2-λ_1 is 100 nm and λ_1 is 550 nm, the coherence length is just 3.6 µm! That is why the mirror M2 is mounted onto a translation stage.

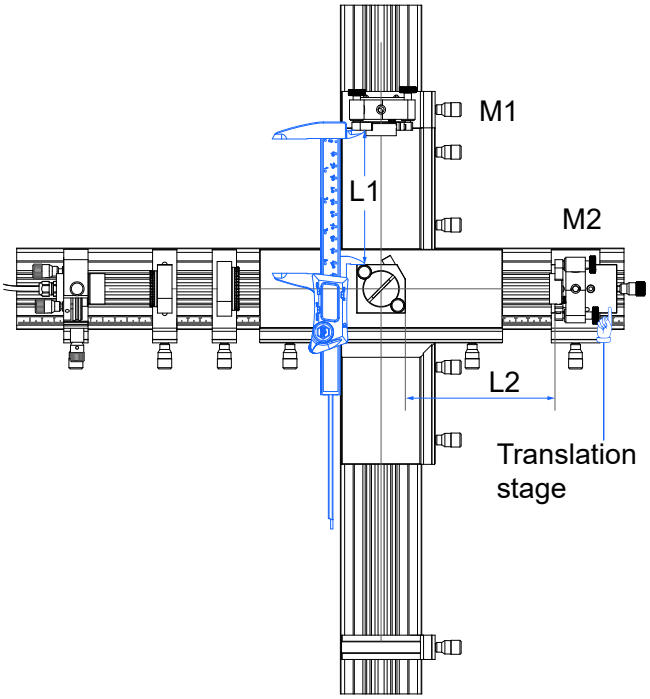

Fig. 33: Alignment of the white light interferometer

The mirror M1 is moved into mechanical contact with the carrier cross piece, which is considered now as reference. With the provided vernier we measure a distance of 111.8 mm. One would assume that L2 should be the same value.

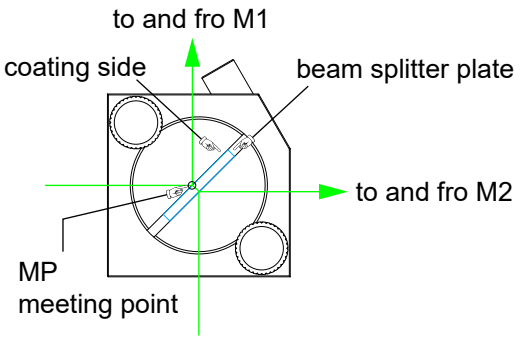

Fig. 34: Analysis of the individual optical paths

However, the ray path analysis shown in Fig. 34 tells us, that although the mechanical distance to M2 is the same as to M1, the optical paths are different, since the beam to M1 is reflected at the coating side of the beam splitter plate, whereas the beam to M2 travels twice through the tilted plate

with a thickness of 2.1 mm before it reaches the meeting point (MP) with the beam from M1 (small circle in Fig. 34). Thus the mechanical distance L2 should be reduced by this amount which can be calculated. The index of refraction is 1.45 and the plate thickness is 2.1 mm. Apparently, the value will be in the mm range, however within the travel range of the translation stage.

By using the vernier, we set the distance L_2 to L_1-2.8 mm, which is 109 mm. Before that, we make sure that the translation stage is in the middle of its travel range. Now we observe the translucent screen and align the mirror M1 and M2 such, that the both crosses perfectly overlap. Tweaking a bit the translation stage and suddenly an interference pattern occurs!

The range of turning the set screw is just a few degrees. We should keep in mind, that the coherence length is around 3 µm only and one turn (360°) of the knob shifts the stage already by 250 µm. It can be seen, that the colour of the interference pattern changes, when we slightly change the position of the translation stage. From a regular Michelson interferometer we know that destructive interference shows dark fringes, however, in this case when the constructive fringes are blue, the remaining background light does not contain any blue and the remaining red and green appear as yellow. The Fig. 35 to Fig. 37 show a collection of different coloured interference fringes. However, there exists a position of the translation stage, where the optical distance of both interferometer arms are exactly the same and white interference fringes should be observable.

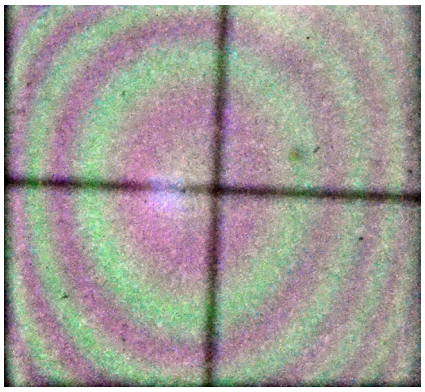

Fig. 35: Red fringes on a green background

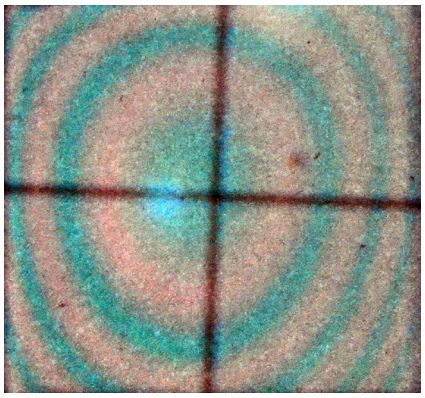

Fig. 36: Green fringes on an orange background

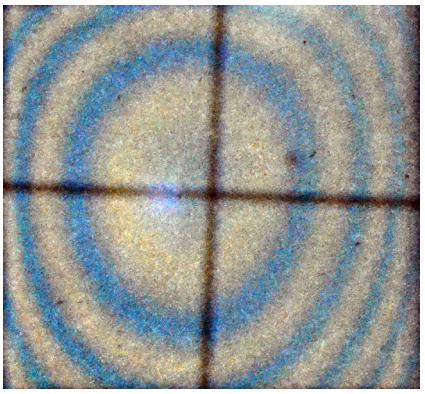

Fig. 37: Blue fringes on a yellow background

4.3 Audible fringe detection

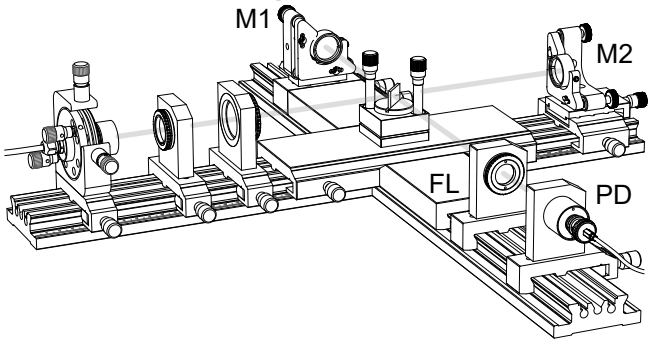

Another nice method to find the position of M2 fo which L1 equals L2 is to use an audible method. Instead the translucent screen we add a photodetector. In front of the photodetector the focusing lens with f=60 is placed. At the beginning the distance should be chosen to be around 40 mm. The photodetector is connected via a BNC cable to the pre-amplifier (see Fig. 23) which is connected to an active speaker. Any changes of the light intensity hitting the detector will be amplified and made audible by the speaker. Since at the beginning the pre-amplifier as well as the speaker will be operated with highest gain, all other light sources in the room must be switched off!. When you are sweeping over the point of equal optical path lengths you will hear a chirp which frequency depends on the sweep speed (turning the knob of the translation stage). Exchange the photodiode against the translucent screen and you will see the interference pattern!

4.4 Mach Zehnder Interferometer

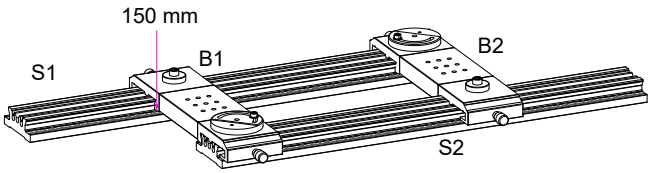

Fig. 38: Basic structure of the Mach Zehnder Interferometer

The experiments starts with the composition of the basic structure consisting of 2 rails S1 and S2 each with 500 mm length and the two bridge connectors B1 and B2. B1 is positioned at 150 mm of the rails S1 and the second bridge at the end of S1. The rail S2 is located at the beginning of S2 as shown in the Fig. 38.

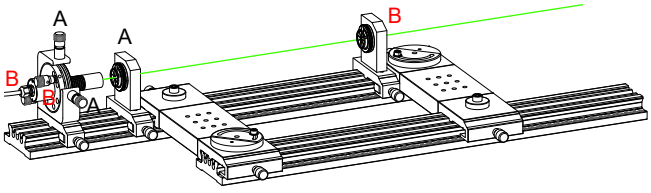

Fig. 39: Aligning the green laser

Within the next step the beam of the green laser is aligned with respect to the mechanical axis of the setup. For this purpose we are using the provided iris which is plugged into a mounting plate. The iris is moved to the position B and the green laser is aligned by using the adjustment screws (B). After that, the iris is brought into the position A and aligned by the adjustment screws (A). These steps are repeated until there is no more deviation to the iris hole in both positions A and B.

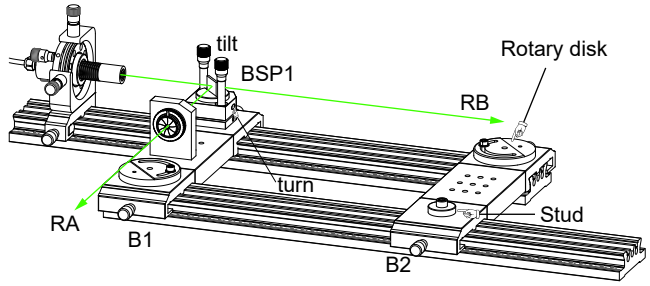

Fig. 40: Placing and aligning the first beam splitter plate

The first adjustable beam splitter unit BSP1 is fixed to the 25 mm stud of the first bridge (B1). Now the iris is plugged into the mounting plate with the two 4 mm fixing pins. The centre hole of the iris is the reference for the deviated beam (RA). By using the alignment screws of the BSP1 the beam is laced through the iris hole.

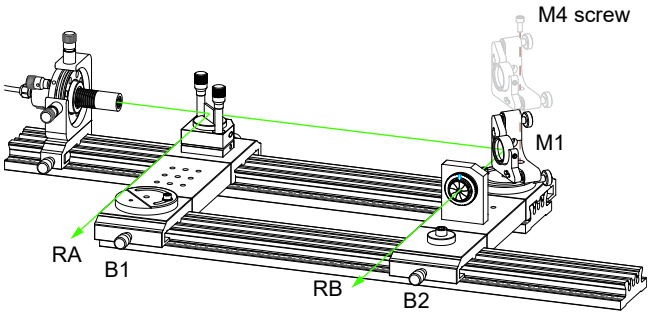

Fig. 41: Inserting the first beam bending mirror

One of the adjustment holder with interferometer mirror is set onto the rotary disk of B2 and locked with the M4 screw. Subsequently the iris is moved from the bridge B1 to B2 and the Beam RB is laced through the iris hole by aligning the mirror M1.

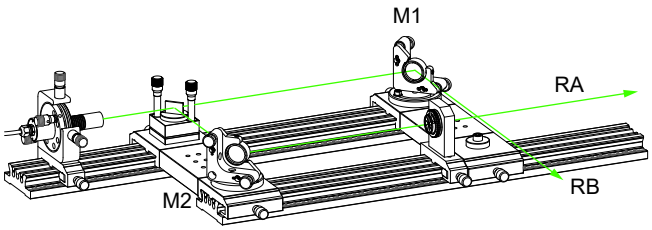

Fig. 42: Inserting bending mirror M2

By means of the mirror M2, the by 90° bended beam RA is laced through the iris which is now positioned by using a mounting plate on a carrier.

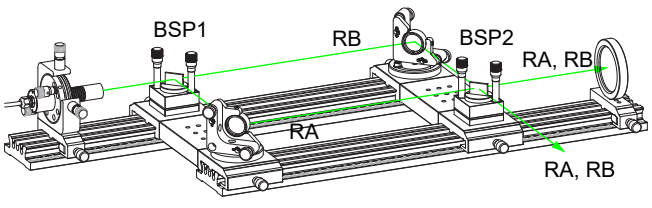

Fig. 43: Adding the second beam splitter BSP2

The setup is completed after adding the beam splitter BSP2, which actually works as beam combiner. The beam RA passes the beam splitter plate of BSP2 and undergoes a slight parallel offset. It should hit the translucent screen in its centre. However, the beam RB is reflected from the plate and its direction depends on the alignment of the plate. By using the alignment screws of the BSP2 the spot of RB is aligned to overlap with the spot of RA on the translucent screen. Both beams RA and RB must propagate collinear within each other for best interference. This is checked by looking to the overlap in 1 or 2 m distance on the screen. If not, there are a manifold of possible alignment strategies.

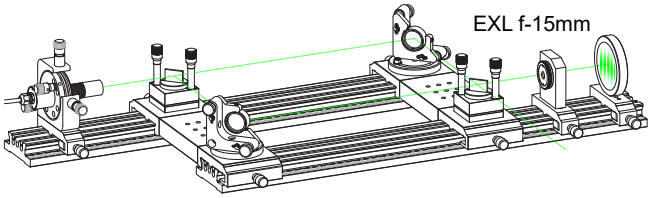

Fig. 44: Observation of the interference pattern

The goal is to achieve a crisp and clean interference pattern centred to the screen. For this purpose we add the expansion lens EXL f-15 mm in front of the screen and obtain an enlarged interference pattern. If the contrast may be to low, the green laser diode may drifted to multimode emission. Shortly change the injection current and the laser jumps back to single mode emission.

4.5 Mach Zehnder with Vacuum Cell

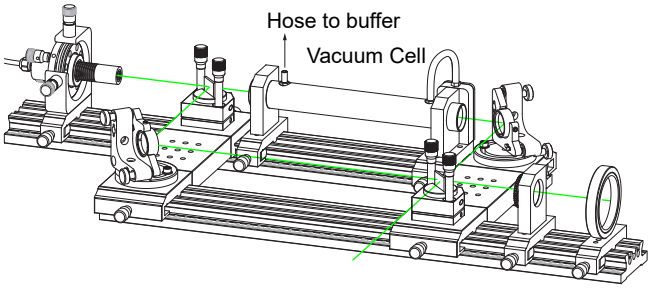

Once the alignment has been done, the vacuum cell is inserted. By means of the provided patch hoses the cell is connected to the buffer, which itself is a 100 m long hose which is coiled to a drum. This hose is further connected to the vacuum controller (see full picture on page 14).
The aim of the subsequent measurements is the determination of the index of refraction of air, firstly by the interferometer and secondly by applying the Edlen formula. A possible measurement table may look like this one:

P1 [hPa]	P2 [hPa]	Counted Fringes	T [°C]	H[%]
air	air-50 hPa			

The measurement start with the local air pressure read from the controller. The value of the set pressure is set, let's say less 50 hPa. During the pump is running the number of fringes is counted by eye. It is helpful to use a stylus to point on the screen as reference. For each measurement the actual pressure, temperature and humidity is noted.
From the number of counted fringes the change of the optical path is calculated by multiplying with λ/2, whereby λ is 532 nm. The length L_0 of the vacuum zone of the cell is known (187 mm, Fig. 27). From these informations we can determine the index of refraction of air as function of the air pressure. Finally, the comparison with the values calculated by using the Edlen formula should yield a good approximation.